

Systematic Two-band Model Calculations of the GMR Effect with Metallic and Nonmetallic Spacers and with Impurities*

O. Gebele^{1†}, M. Böhm^{1‡}, U. Krey^{1§} and S. Krompiewski²

¹ Institut für Physik II der Universität, 93040 Regensburg, Germany

² Institute of Molecular Physics, P.A.N., 60-179 Poznań, Poland

received: 12/07/1999; revised 3/12/1999; accepted 24/2/2000

Abstract

By a semi-empirical Green's function method we calculate conductances and the corresponding Giant Magneto-Resistance effects (GMR) of two metallic ferromagnetic films separated by different spacers, metallic and non-metallic ones, in a simplified model on a *sc* lattice, in CPP and CIP geometries (i.e. current perpendicular or parallel to the planes), without impurities, or with interface- or bulk impurities. The electronic structure of the systems is approximated by two hybridized orbitals per atom, to mimic s-bands and d-bands and their hybridization.

We show that such calculations usually give rough estimates only, but of the correct order of magnitude; in particular, the predictions on the impurity effects depend strongly on the model parameters. One of our main results is the prediction of huge CPP-GMR effects for *non-metallic* spacers in the ballistic limit.

PACS: 75.70.-i – Magnetic films and multilayers; 73.40.GK – Tunneling; 73.40.Ns – Metal-nonmetal contacts

*Based on the *Diploma Thesis* of O. Gebele, Regensburg 1998

†present address: Gebele@tu-harburg.de

‡present address: mBoehm@wila-verlag.de

§Corresponding author, FAX (xx49) 941 943-4544, e-mail uwe.krey@physik.uni-regensburg.de

1 Introduction

The presence of giant magneto-resistance effects in trilayer systems consisting of two ferromagnetic metallic layers – source and drain – separated by a non-magnetic or anti-ferromagnetic crystalline metallic spacer is meanwhile well-known [1, 2]. Recently also non-crystalline and non-metallic spacers have been considered [3, 4, 5], i.e. there is renewed interest in spin-polarized tunneling through semi-conducting or non-conducting spacers [6, 7, 8], based on the perspective of new applications in magneto-electronic technology, e.g. for magnetic-field sensors, spin-valve transistors [9] or spin-polarized field-effect transistors [10, 11].

In [12, 13] spin-valve properties of ferromagnet/insulator/ferromagnet junctions were studied, and [14] presents a first *ab initio* calculation of the *one-particle* electronic and magnetic properties of FM/NM/FM tunneling structures, with FM=Fe, and NM=Ge and GaAs.

However concerning the GMR effect, which is based on *two-particle* properties, equally accurate calculations for FM/NM/FM systems, particularly in the CPP geometry, apparently could only be performed without impurities, [15]. For systems with *metallic* spacers one should mention at the same time the calculations of Tsymbal and Pettifor, [16], or Mathon, [17], where also fully realistic calculations have been performed, but again with phenomenological assumptions for the impurity scattering, [16], or with no impurities at all, [17]. Furthermore, in a two-band tight-binding approximation, two of the present authors, [18], have already treated systems, where one or two of the ferromagnet-spacer interfaces were decorated with ultrathin non-metallic layers, but again with translational invariance within the planes. In this approximation, the two bands mentioned above describe the s- and d-electrons and their hybridization, or the conduction and valence band in case of a non-metallic spacer.

In the ferromagnetic metals, the parameters of the d-band are of course spin-dependent.

Since in [18] the method for the calculation of the resistivities turned out to be extremely flexible and accurate, we extend it in the present paper to a systematic survey of the magnetoresistivity of trilayers of two ferromagnetic sandwiches separated by different non-magnetic spacers, metallic and non-metallic ones, with impurities of various kind, and

without impurities, in CIP and CPP geometries, but within a simplified semi-empirical hybridized two-band model.

We stress that our approach is rigorous in principle, numerically very accurate, and avoids the Coherent Potential Approximation (CPA), which is often applied to disordered systems, but difficult to control.

As already mentioned, there exists already a large body of theoretical calculations on the GMR of magnetic multilayer systems. For systems with metallic spacers and without impurities our simplified two-band model calculations, to be presented below, can of course not compete – and this is also not at all intended – with the much more ambitious and cumbersome calculations mentioned above e.g. those of [17], who performed fully realistic calculations of the CPP- and CIP-GMR for Co/Cu/Co/Cu and Fe/Cr/Fe/Cr multilayers with ideal leads made of Cu resp. Cr, in the ballistic, Ohmic, and Anderson-localized regimes corresponding to the cases of no-disorder resp. certain cases of one-dimensional disorder, i.e. with respect to the stacking of the planes, but without impurities. There exist more such ambitious calculations, e.g. the seminal paper of Schep *et al.*, [19], and other publications, which also in principle would have earned citing but which are omitted on lack of space. In this respect the purpose of our paper is, instead, to study in some detail the question, *to which extent* simplified models as the present one are able (or not) to reproduce those results.

On the other hand, with impurities, on which we concentrate, similar extensive calculations of corresponding rigour do not yet exist, to our knowledge. In fact, concerning the influence of impurities, the *methods* of our calculation have already been presented in the paper of Asano *et al.*, [20]. However, rigorous calculations with impurities are so demanding that those authors, although they wrote already down the formalism for a *two-band model*, published numerical results only for *one-band* cases.

Here we present results obtained with the two-band model within the formalism of [20]. For a *nonmetallic* spacer it is actually necessary to consider at least two orbitals per atom to simulate the valence and conduction bands, respectively, but also for ferromagnetic or non-magnetic 3d-*metals* it is a natural requirement to include a second band with the intention to mimic as far as possible the d-electrons in addition to the s-states. Namely, the d-electrons are not only responsible

for the magnetic properties, but also for a large part of the resistivity, due to *Mott's s-d-scattering mechanism*. Therefore it is also important to include not only two bands, but also realistic values for the *s-d hybridization*.

This should give enough motivation to our two-band calculation; but we stress again that these calculations should be considered as model calculations and are not intended to replace fully realistic calculations, as far as they are possible already now, e.g. [17], or in future. In fact, it turns out that the present two-band model calculations will be able to give estimates of the GMR, which yield the correct order of magnitude, but not more. Further, concerning the impurity effects, it turns out that certain contradictory results (see below) concerning essential trends depend strongly on the model-parameters, so that again, now with impurities, completely realistic calculations cannot be avoided: Unfortunately, such calculations, where the impurities are treated with the same kind of rigour as the electronic structure of the pure system itself, are apparently not yet possible, [21]–[25].

On the other hand, one of our most remarkable predictions, which should not be overlooked and can be stated already from the present model calculations, is that a large enhancement of the CPP-GMR may happen, if *nonmetallic spacers* of increasing thickness are used. Here it is of course required that the thickness of the nonmetallic spacer remains smaller than the dephasing length for inelastic scattering; i.e. one should remain in the ballistic limit.

In the following sections we present the basic theory and then the results of our survey, which is followed at the end by a section presenting our conclusions.

2 Basic definitions

2.1 Systems

Our systems are defined in Fig. 1 and Fig. 2 for the CPP and CIP geometries, respectively.

We start with metallic 'ideal leads' on the left-hand side and right-hand-side, respectively, followed – in the CPP geometry – by three monolayers of ferromagnetic metal F_1 resp. F_2 , with n_s spacer mono-

layers inbetween. In the CPP geometry all layers have a quadratic cross-section of $M \times M$ square-lattice unit cells.

For the CIP geometry, the natural definition of our systems is similar and explained by Fig. 2.

The electronic structure of our systems is described by the following tight-binding Hamiltonian :

$$\begin{aligned}
\mathcal{H} = & \sum_{l,i} E_{l,i}^s \sum_{\sigma} \hat{c}_{l,i,\sigma}^+ \hat{c}_{l,i,\sigma} + \sum_{l,i} \sum_{l',i'} t_{l,i,l',i'}^s \sum_{\sigma} \hat{c}_{l,i,\sigma}^+ \hat{c}_{l',i',\sigma} \\
& + \sum_{l,i} \sum_{\sigma} E_{l,i,\sigma}^d \hat{d}_{l,i,\sigma}^+ \hat{d}_{l,i,\sigma} + \sum_{l,i} \sum_{l',i'} t_{l,i,l',i'}^d \sum_{\sigma} \hat{d}_{l,i,\sigma}^+ \hat{d}_{l',i',\sigma} \\
& + \sum_{li} V_{l,i}^{s,d} \sum_{\sigma} (\hat{d}_{l,i,\sigma}^+ \hat{c}_{l,i,\sigma} + \hat{c}_{l,i,\sigma}^+ \hat{d}_{l,i,\sigma}) .
\end{aligned}$$

Here $\hat{c}_{l,i,\sigma}^+$ and $\hat{c}_{l,i,\sigma}$ denote creation and destruction operators of an s-electron occupying the site l in plane i with spin σ . The corresponding operators for d-electrons are $\hat{d}_{l,i,\sigma}^+$ and $\hat{d}_{l,i,\sigma}$. The band-energy parameters are $E_{l,i}^s$ for the s-states, which do not depend on the spin σ , and $E_{l,i,\sigma}^d$, which are spin-dependent, for the d-states. The hopping-matrix elements for s- and d-states are $t_{l,i,l',i'}^s$ and $t_{l,i,l',i'}^d$, and the local s-d-hybridization is given by $V_{l,i}^{s,d}$.

Of course, taking more bands into account, i.e. all five d-bands, the 4s-band and the three 4p-bands, and adding the spin dependence, we could have tried to fit the band structure of realistic systems as far as possible, see e.g. [26]; but this is *not* our purpose, since we try to remain semi-quantitative and study only the essential trends. Particularly, in view of the still much simplified band structure, we also use typical simplifications in the description of the impurities, see below. But in principle, within our formalism, more rigour in both respects would be possible, but only at the cost of excessive computing.

For the following, \mathcal{H} is written in matrix representation with respect to an orthonormal basis by replacing the creation and annihilation operators by the corresponding ket- and bra-vectors, respectively, such that $\mathcal{H} \rightarrow \hat{H}$, e.g. by $\hat{d}_{l,i,\sigma}^+ \hat{c}_{l,i,\sigma} \rightarrow |d, l, i, \sigma\rangle \langle s, l, i, \sigma|$.

2.2 Resolvent operators and Kubo formula

For the calculation of the conductances we use the formalism of Fisher and Lee, [27]. Therefore, we need the following matrix elements of the

advanced and retarded resolvent operators $\hat{G}^\pm := \{E \pm i0^+ - \hat{H}\}^{-1}$:

$$G^\pm(i, i')_{\alpha, l, \sigma; \alpha', l', \sigma'} = \langle \alpha, i, l, \sigma | \{E \pm i0^+ - \hat{H}\}^{-1} | \alpha', i', l', \sigma' \rangle . \quad (1)$$

Here the index α counts the orbitals, e.g. $\alpha = s$ or d . As usual, we also call these matrices 'Green's operators', and $i0^+$ is a positive imaginary infinitesimal, such that the matrix-inverse in this equation always exists in our approach.

For auxiliary purposes we need the 'left-sided' and 'right-sided' Green's operators G^L and G^R , e.g.

$$G^L(i_0)_{\alpha, l, \sigma; \alpha', l', \sigma'} := \langle \alpha, i_0, l, \sigma | \{E + i0^+ - \hat{H}_L^{i_0}\}^{-1} | \alpha', i_0, l', \sigma' \rangle . \quad (2)$$

Here $\hat{H}_L^{i_0}$ denotes the Hamiltonian for a system, in which all planes $i > i_0$ are deleted; $G^R(i_0)$ is defined in a similar way with $E + i0^+ - \hat{H}_R^{i_0}$, where $H_R^{i_0}$ is the Hamiltonian of a system with all planes $i < i_0$ deleted. G^L and G^R are obtained by *recursion*, e.g. G^L by recursion from the left, i.e.

$$G^L(i_0) = [\hat{g}(i_0)^{-1} - \hat{T}G^L(i_0 - 1)\hat{T}]^{-1} . \quad (3)$$

$\hat{g}(i_0)$ is the resolvent of the isolated plane i_0 ; \hat{T} is the matrix describing the 'hopping' from plane to plane.

From this one gets finally the two desired resolvent operators

$$G(i, i) = [\hat{g}(i)^{-1} - \hat{T}G^L(i - 1)\hat{T} - \hat{T}G^R(i + 1)\hat{T}]^{-1} \quad (4)$$

and

$$G(i, i + 1) = G(i, i)\hat{T}G^R(i + 1) , \quad (5)$$

which are needed for the conductance, see below. Here the plane i ($= i_0$) is arbitrary, since under stationary conditions through any of the planes the same amount of current is flowing.

Finally, with the definition

$$\tilde{G}(i, i') := \frac{1}{2i} [G^-(i, i') - G^+(i, i')] \quad (6)$$

one gets the conductance from the Kubo-formula, [27]:

$$\Gamma_\sigma = \frac{4e^2}{h} \text{Tr}_{l, \alpha} [\tilde{G}(i, i)\hat{T}\tilde{G}(i + 1, i + 1)\hat{T} - \hat{T}\tilde{G}(i, i - 1)\hat{T}\tilde{G}(i, i - 1)] , \quad (7)$$

where the trace $\text{Tr}_{l,\alpha}$ is performed with respect to the orbitals $\alpha = s, d$, and with respect to the sites l of the atoms of a given plane, whereas the spin-index $\sigma (= \sigma')$ is kept fixed. Here e is the electronic charge, and h is Planck's constant.

The GMR effect is defined by the equation

$$\text{GMR} = \frac{\Gamma_{\sigma=\uparrow}^{++} + \Gamma_{\sigma=\downarrow}^{++}}{\Gamma_{\sigma=\uparrow}^{+-} + \Gamma_{\sigma=\downarrow}^{+-}} - 1 = \frac{\Gamma^{++}}{\Gamma^{+-}} - 1 . \quad (8)$$

Here the superscripts $(++)$ resp. $(+-)$ denote *mutually parallel* resp. *antiparallel* magnetizations of the two ferromagnetic sandwiches. Since we neglect spin-flip scattering altogether, the conductances are of course additively composed out of the separate contributions from majority and minority spins, respectively, as denoted in the formula.

We have performed real-space (x-space) and k-space calculations. In the x-space calculations each layer consists of $M \times M = 10 \times 10$ atoms with free boundary conditions, [28]. Here the matrices are of size 200×200 , again for given $\sigma (= \sigma')$. Impurities can be added at will, which is important below.

In our k -space calculations, which are only performed in the CPP case and without impurities, the planes are infinitely extended. Here, in the trace of equation (7), in the k -space representation, the sum over l is replaced by the corresponding sum over \vec{k} -vectors in the two-dimensional Brillouin zone, since the two-dimensional vector \vec{k}_{\parallel} is now 'a good quantum number', i.e. there is translational invariance in the planes. This summation, or the corresponding integral, is approximated extremely accurately by a Cunningham formula, [29], with $\sim 10^6$ \vec{k}_{\parallel} -points, for which the matrix elements of the Green's operators can be calculated separately without difficulty and extremely accurately. (All numerical evaluations have been performed with Cunningham's accuracy parameter $m = 10$ or 11).

2.3 Model parameters

For the models considered, we have chosen four parameter sets: Two parameter sets, (i) and (ii), correspond to a *metallic* spacer and mimic the main features of trilayers composed of Co as ferromagnetic metals and Cu as nonmagnetic metallic spacer material (see below), whereas

the third and fourth parameter sets, (iii) and (iv), correspond again to Co ferromagnets, but with a *non-metallic* spacer.

Concerning the sets (i) and (ii), we note that, as already mentioned, they are constructed to reflect the two main features of Co and Cu as far as possible in our simplified two-band model: The two features are

- the similarity of the s-bands of Co and Cu, and
- the similarity of the d-bands of Cu and the 'majority-spin' d-bands of Co.

This qualitative similarity is obvious from Fig. 3, which presents results obtained by Mathon *et al.*, [30]. The parameter sets (i) and (ii) are in fact derived from rough fits to *the overall band-structure of Co* – parameter set (i), see Fig. 4a – respectively to *the overall structure of the DOS for Co* – parameter set (ii), see Fig. 4b. But these fits are rather crude anyway, and so the derivation is not emphasized. The values are given in Table 1 and Table 2, respectively, [31].

In Tables 3 and 4, the parameter sets (iii) and (iv) are given, which correspond to *nonmetallic* spacers ('Isolator 1 and 2', respectively). The parameters of the ferromagnet correspond to case (i), with $E_F = -2.8$.

The notions 'indirect energy gap' and 'direct energy gap', which are used in the table captions of Table 3 and 4, respectively, refer to Fig. 5: For parameter set (iii) there is an '*indirect energy gap*', since the valence-band maximum is at $k_{[111]} = (\pi/a)\sqrt{3}$ with an energy -2.81, which is slightly below the Fermi energy $E_F = -2.80$, whereas the minimum of the conduction-band energy is at $k_{[111]} = 0$ with $E = -2.79$. These numbers refer to the first line of the three parameter sets of Table 3.

On the other hand, with parameter set (iv), also with $E_F = -2.8$, there is a *direct* energy gap at $k_{[111]} = 0.814$, i.e. at the *arrow* in the r.h.s. of Fig. 5. In both figures, and in the results presented below, the uppermost line, i.e. with the smallest gap, of Table 3 and Table 4 has been used.

2.4 Impurity models

We consider a) bulk impurities and b) interface impurities.

In case a), we have considered *bulk impurities* only in the spacer, and exclusively nonmagnetic ones, which are modelled by adding to the parameter E_d of the single-site d-band energy a *Gaussian spatial noise* proportional to a 'disorder strength' σ_r , namely

$$E_d \rightarrow E_d + \sigma_r \cdot n_l^{\text{Gauss}}. \quad (9)$$

Here the n_l^{Gauss} , where l enumerates the different spacer atoms, are independent random numbers distributed according to a 'Gaussian' with average 0 and variance 1; the parameters of the s-bands remain unchanged.

These assumptions for our bulk impurities are of course rather schematic, i.e. these are the same simplified assumptions e.g. of Asano *et al.*, [20]. But principally one might have been more ambitious and might have considered e.g. specific magnetic impurities. Such calculations are of course always possible within our formalism, [32, 33], and have partially been performed in course of the diploma work of the first one of the present authors; however, as a first step, and since the results with the magnetic impurities were not particularly exciting and have not been documented, also because of lack of space, we keep at present to our simplified description of the impurities. This seems also justified in view of the simplifications made for the band structure and for the geometry of our systems.

Concerning case b), the *interface impurities* are defined as follows : For every ferromagnet-spacer interface, in each of the two boundary layers of the interface there are n atoms (out of $M \times M$) selected at random and replaced by atoms of the other kind.

For impure systems we have of course *averaged* over a large number of different samples, see the figures below; this leads to the 'averages with error bars' in the results presented in the following section.

3 Results

3.1 CPP-GMR

3.1.1 CPP-GMR; no impurities

At first we describe the results obtained without impurities obtained in the CPP case ('current perpendicular to the planes'). In Fig. 6

and Fig. 7 the results of k-space calculations with model parameters (i) and (ii) are presented, for variable thickness n_s of the 'metallic spacer'. Interestingly, in both cases there is a slight but significant spatial oscillation of the GMR as a function of n_s ; in case (i) the GMR oscillates between ~ 70 and ~ 80 % with a quasiperiod of $\lambda \approx 5$ monolayers (ML); in case (ii) the oscillation of the GMR is between ~ 47 and ~ 51 % with $\lambda \approx 3$. Here one can explicitly see that the conductance is *ballistic* from the fact that on average the conductances hardly depend on n_s in the limit $n_s \rightarrow \infty$; in contrast, in case of *Ohmic* behaviour, one would expect that the conductances converge to 0, namely $\propto n_s^{-1}$, as soon as n_s becomes larger than the relevant "scattering length" for diffusive elastic or inelastic scattering, [17].

The reason for the spatially oscillating behaviour of the GMR are tiny oscillations of the conductances Γ_{\uparrow}^{++} and Γ_{\downarrow}^{++} , which are visible in the plots on the r.h.s. of the preceding figures. These oscillations are caused by our treatment of the ideal leads: In fact, for the ideal leads we have always used the same parameters as within the 'Cu' spacer, but usually – with exceptions mentioned below – for the pure system the s-d-hybridization has been neglected in the ideal leads (but not in the spacer). The reason for this neglect is mainly technical, since in case of neglected hybridization we can directly express the matrix elements of the Green's operators $G^L(\vec{k}, i)$ and $G^R(\vec{k}, i)$ at the boundary layers from the ideal lead to the ferromagnetic by simple *analytical* expressions, whereas the numerical calculation is much harder if the s-d-hybridization is taken into account already in the ideal leads, by which the above-mentioned tiny oscillations vanish. What is, however, more important: In this way we have made explicit that the properties of the ideal lead really matter, which is not astonishing with 'ballistic electrons', where the 'contact resistance' from the ideal leads to the system under study plays an important role.

As a first consequence one can learn from this study that it is a mistake to speak of 'the ideal lead' as a uniquely defined entity: In ballistic experiments there are different ideal leads, and it is necessary to characterize them, too, as already stressed in a recent book on electronic transport in mesoscopic systems, [34].

It is also interesting at this place to contrast the different, i.e. parameter-dependent, results of our Fig. 6 and Fig. 7 with the cor-

responding results found by the much more ambitious *ab initio* calculations of [17] and [19]. These authors find values of the CPP-GMR for Co/Cu-multilayers amounting to ~ 150 %. Moreover, for the conductances $\Gamma/M^2[e^2/h]$, instead of our values 0.8; 0.3; and 0.2 (Fig. 6) resp. 0.45; 0.2; and 0.15 (Fig. 7) for the cases $(++,\uparrow)$, $(++,\downarrow)$, and $(+-)$, respectively, they find values of Γ corresponding to $0.43\cdot 10^{15}$, $0.25\cdot 10^{15}$, and $0.165\cdot 10^{15} \Omega^{-1} m^{-2}$, i.e. $\Gamma/M^2[e^2/h] = 0.67, 0.39, \text{ and } 0.26$.

As a conclusion, our values are correct concerning the order of the three conductances, and their order of magnitude, but not more. This is exactly what can be expected.

3.1.2 CPP-GMR; bulk impurities

We would like to stress at this place that with impurities, all calculations have been performed in the *real* lattice space, with cross sections of $M \times M = 10 \times 10$ sites, *free* boundary conditions, in the perpendicular directions, instead of *periodic* ones, and with complete s-d-hybridization everywhere, i.e. now always *including* the ideal leads.

In Fig. 8 and Fig. 9, for $n_s = 3$ and the parameters (i) and (ii), respectively, our results for the GMR and the conductances are presented over the strength of the disorder, i.e. over the standard deviation σ_r in equation (9). For the parameter set (i), Fig. 8, one obtains first a rapid *decrease* of the GMR from $\text{GMR} \approx 1.15$ to $\text{GMR} \approx 0.45$, when σ_r increases from 0 to 1, followed by a plateau behaviour with further increase of σ_r . Concerning the behaviour of Γ_σ^{++} , Γ_σ^{--} , and Γ_σ^{+-} , one can see from the r.h.s. of Fig. 8 that the GMR reflects essentially the behaviour of Γ_\uparrow^{++} .

For the parameter set (ii), Fig. 9, there is also at first a rapid decrease from $\text{GMR} \approx 0.37$ at $\sigma_r = 0$ down to $\text{GMR} \approx 0.15$ at $\sigma_r \approx 1$, but with a further increase of σ_r there is now a significant *re-increase* of GMR back to $\sigma_r \approx 0.22$ for $\sigma_r \approx 6$. In fact, in this case the behaviour of the conductances, which are plotted on the r.h.s. of Fig. 9, is significantly different and more subtle than that of Fig. 8. In particular, the results of Fig. 9 differ from what in [20] the authors have obtained from a simple one-band model.

So from these two figures, Fig. 8 and Fig. 9, concerning the dependence on the strength of disorder σ_r , one may only conclude that at first a rapid decrease of $\text{GMR}(\sigma_r)$ from its value at $\sigma_r = 0$ to

GMR(1) $\approx 0.4 \cdot \text{GMR}(0)$ would be typical; this qualitative behaviour seems to be essentially parameter-independent; but for $\sigma_r > 1$ a quantitative calculation is hardly avoidable, [22, 35].

The reason for the common 'decreasing behaviour' for $\sigma_r \lesssim 1$ is the following: In this case, an increase of σ_r leads to an effective reduction of the number of open channels for coherent motion of an electron from one plane to the next. This reduction concerns mainly Γ_{\uparrow}^{++} and therefore leads to a *decrease* of the GMR, since the majority-spin d-electrons, *without* impurities, would not feel any potential-variation at all.

In this connection, a very recent paper of Bruno *et al.*, [36], should be mentioned: There it is shown that the conductance of systems with impurities can be decomposed into two parts, a 'diffusive' part, arising from scattering processes, where the in-plane \vec{k}_{\parallel} -vector is not conserved, as is generically always the case for the present systems with impurities and free-boundary conditions, and a 'ballistic' part, to which only those processes contribute, where the \vec{k}_{\parallel} -vector is the same for the incoming and outgoing waves. The diffusive part (resp. ballistic part) always dominates the conductance, as long as the spacer length is much shorter (resp. much longer) than the *scattering length* l_s of the system. According to [36], l_s should be of the order of several 100 lattice spacings under similar conditions as in the present work. So in our systems with impurities, where n_s is very small ($n_s = 3$), always the *diffusive* part of the conductance dominates.

3.1.3 CPP-GMR; interface impurities

In the following Fig. 10 and Fig. 11 the number n of impurities is varied between $n = 0$ and $n = 80$ for every interface layer (remember that per interface, two layers are involved, with 100 sites per layer; so we have $2 \times n$ impurity sites out of 200 per interface, occupied by a 'wrong atom').

For the parameter set (i), Fig. 10, the GMR *decreases* with increasing number of impurities, whereas for parameter set (ii), Fig. 11, there is again the opposite behaviour: Here the GMR *increases* with increasing number of impurities.

This difference contains again an important statement in itself, which should be particularly relevant to the experimentalist :

Without a precise calculation for a specific model one cannot predict whether an increase of the number of interface impurities will lead to an increase or a decrease of the GMR.

3.2 CIP-GMR

3.2.1 CIP-GMR; no impurities

The formalisms of the preceding sections can also be applied on equal footings to the situation, where the current is in the direction of the planes (CIP geometry, see Fig. 2). The ideal leads have cross-sections of $\Delta z \times \Delta y = N \times M$ with $N = 6 + n_s$, see below, while the CIP-conductor consists again of $\Delta z = N$ monolayers of length $L = \Delta x = 10$ and width $\Delta y = M = 10$, namely two ferromagnetic sandwiches of height $\Delta z = 3$ and inbetween a spacer sandwich of $\Delta z = n_s$. Again we consider at first the situation without impurities; however in this geometry we have applied the x-space calculation right from the beginning, i.e. with cross sections of size 10×10 and with *free* boundaries, although with respect to the coordinate y one could have still performed a Fourier transform. Moreover, as for the CPP geometry without impurities, this time the s-d-hybridization has been switched off for the lead wires.

In Fig. 12 and Fig. 13, the ballistic CIP conductances are plotted as a function of n_s , for the parameter sets (i) and (ii), respectively. In the first case, with increasing n_s the conductances Γ/M^2 rise, because the spacer cross section increases, the limiting value given by the "shunting" through the Cu spacer. The GMR shows irregular oscillations as a function of n_s ; these oscillations change with the boundary conditions, the geometry, and the material, and the results are more than one order of magnitude smaller than for the CPP geometry, [37, 38, 39]. Note that with parameter set (i), the GMR is even negative on average over n_s , which is not observed experimentally. By discrete Fourier transformation of GMR with respect to n_s , [40], we would get maxima in the Fourier spectrum at periods of 2.5, 4.6 and 8.33 monolayers (ML) from parameter set (i), Fig. 12, and 2.27 and 5 ML from (ii), Fig. 13.

3.2.2 CIP-GMR; bulk impurities

In case of bulk impurities, we have considered a system with $n_s = 4$, i.e. $N = L = 10$. The results are presented as a function of σ_r , the param-

eter characterizing the 'strength of the disorder' according to Eq. (9). Here, in case of the parameter sets (i) and (ii), we find again quite different behaviour in Fig. 14 and 15, respectively: In case of Fig. 14, i.e. for parameter set (i), the GMR *increases* at first from 0 to 0.015, and then for $\sigma_r > 1$ it roughly remains constant with increasing σ_r , whereas in case of the parameter set (ii), i.e. in Fig. 15, there is at first a drastic *decrease* from GMR ~ 0.035 to GMR ~ 0 , and then again a roughly constant value of GMR ~ 0 , [37]. In both cases the *conductances* decrease at first rather fast, and then there is a slow re-increase; but this behaviour is slightly different for the up- and down-spin channels in the $(++)$ -configuration, and for the $(+-)$ -configuration.

So again the behaviour of the GMR as a function of σ_r is hardly predictable without an extensive and completely realistic calculation for a specific model.

3.2.3 CIP-GMR; interface impurities

A somewhat different conclusion refers to the influence of *interface impurities* for the CIP geometry. Here in Fig. 16 and 17 we use the same geometry as in the two preceding figures. The GMR rises significantly up to 50 % impurities - i.e. this time we have the same trend for both models (i) and (ii) -, and then it falls again, which is natural since a system of two *three-ML* ferromagnets separated by a 4-ML-spacer and $x > 50$ % interface impurities is equivalent with two *four-ML* ferromagnets separated by a 2-ML spacer with $x' = (1 - x) < 50$ % interface impurities. Here it should be noted that the majority-spin carriers are hardly influenced by our interface disorder, which is clear since we have assumed that the s-bands and the majority d-bands of our metallic ferromagnets and of the metallic spacers are identical. But it should also be noted that at the above-mentioned maximum the CIP-GMR with *interface* scattering reaches much higher values (e.g. 9% and 8% respectively, for the parameter sets of (i) and (ii)) as with our nonmagnetic impurities in the *bulk*.

4 Non-metallic spacers, CPP geometry

Finally, we come to our most startling result, for the non-metallic spacers, where we have considered metallic ferromagnets as in model (i), but *semi-conducting spacer layers* as in the first line of Tables 3 and 4. The geometrical situation corresponds to the CPP geometry of Fig. 1, with metallic ferromagnets (two-times 3 monolayers) and a variable number n_s of semi-conducting spacer layers, i.e. with a conduction band and a valence band, inbetween. Of course one now expects a strong exponential decrease of all conductances with increasing n_s , but GMR $=(\Gamma^{++}/\Gamma^{+-}) - 1$ may be well defined and even *increase* with increasing n_s , as long as the spacer thickness does not become larger than the 'dephasing scattering length' or 'spin-flip scattering length'.

The calculations have been performed by the highly accurate \vec{k} -space method in reliable numerical accuracy, and we have plotted the conductances and the GMR against the number n_s of spacer layers, calculated in the ballistic limit of perfect phase coherence. In Fig. 18 and Fig. 19 there is now the expected drastic exponential decrease of the conductance, which for our model is *weaker* for Γ^{++} than for Γ^{+-} . (The decay is weakest for Γ_{\downarrow}^{++} , which is reasonable, since the \downarrow d-electrons have a much lower energy gap to the lower edge of the semiconductor conduction band than the \uparrow d-electrons, and with the Γ^{+-} case, in contrast to the Γ^{++} case, there are the additional 'matching' problems at the interface to the second ferromagnet. Note that due to the s-d-hybridization, and with the finite value of t_d , the d-electrons do in any case contribute to the tunneling current.) So this means that in our case, and in the recent calculation of MacLaren *et al.*, [15], to be discussed below, and in contrast to Julliere's assumptions, [7], the tunneling matrix through the semi-conducting spacer is naturally strongly spin-dependent. (The fact that here for Γ^{+-} the exponential decay with the spacer thickness is stronger than for Γ^{++} , depends of course on our model: for other assumptions on the semi-conductor it might be just the other-way round.)

As a consequence, one gets a positive GMR, which *strongly increases* with n_s , e.g. up to GMR $\sim 300\%$ for $n_s \gtrsim 5$ in case of model (iv), Fig. 18, i.e. for the model with the 'direct energy gap'. For the case of model (iii) with the 'indirect gap', Fig. 19, the increase is at first similar,

i.e. for $n_s \lesssim 4$, but then the GMR increases even further to *colossal* values, e.g. GMR $\sim 2500\%$ for $n_s = 7$. However because of the strong exponential decrease of the conductance, and in view of the fact that we have neglected indirect transitions involving phonons, this region is probably beyond experimental realizability, and the results of Fig. 18 and Fig. 19 should not be taken literally, although the numerical accuracy of our calculations seems to be sufficient (In Fig. 18 and Fig. 19, the Cunningham accuracy parameter, see [29], was $m = 10$).

In fact, however, in the already cited recent paper of MacLaren *et al.*, [15], which contains an ambitious realistic LKKR calculation of the ballistic CPP conductances and the corresponding GMR for bcc (001) Fe/ZnSe/Fe trilayers, the conductances of Fig. 3 of that paper resemble very much – almost quantitatively – to the results of our simple model calculation in Fig.19. One only must take into account that in the paper of MacLaren *et al.*, one Zn-Se bcc double-layer is replaced by two monolayers in our simple *sc* two-band model calculation with the parameter set (iii). So here we have an example where a fully realistic ab-initio calculation may be sometimes not necessary after all.

Finally we present at this place additional comments on the seminal paper of Julliere, [7], written already in 1975. Julliere describes the tunneling conductance from the ferromagnetic metallic *source* to a metallic ferromagnetic *drain* through an isolating Al_2O_3 spacer as a product of the densities of states (DOS) of the ferromagnetic source and drain, multiplied by an effective tunneling matrix element. This should be essentially equivalent to our approach, which involves two imaginary parts of Green's function, which represent in principle densities of states. But from the relevant densities of states of the magnetic metals, the contributions of *confined* electrons, which contribute to the DOS, but not to the conductance, should be excluded; such confined states exist e.g. with the Co down-spin electrons, which are strongly reflected at the Cu interfaces; so instead of Julliere's DOS, an 'effective DOS' should be used, and since the reduction factor of the DOS to this 'effective DOS' is spin-dependent, the remaining 'effective tunneling matrix elements', if one uses the original DOS, i.e. Julliere's formula, would in any case depend on the spin, contrary to Julliere's assumption, if applied to systems as $\text{Co}/\text{Al}_2\text{O}_3/\text{Co}$, [41].

In principle, however, our approach is even more explicit, and more

demanding, since it also involves the transfers to (and from) the ideal leads to the ferromagnetic metal, and from the reservoirs to the ideal leads.

In Julliere's TMR experiments, and similar experiments performed at present, the high values of the TMR predicted in the present paper and also in the paper of MacLaren *et al.*, [15], have *not* been observed hitherto. However one should stress that our insulating layers are extremely thin (from 1 to 15 monolayers only) with ideal interfaces, whereas the experimental thicknesses of the Al_2O_3 spacers are larger and with rougher interfaces, so that in that case spin-channel mixing might play a role, particularly if on the metallic side of the interface the transverse spin components are almost as probable as the z -components. The band-structure, e.g. that of the semi-conductors involved, is also crucial, since the exponential decay with the spacer-thickness should be weaker for Γ^{++} than for Γ^{+-} , i.e. the semi-conducting compounds involved should have properties similar to those of our present models, or to the Fe/ZnSe/Fe-system studied by MacLaren *et al.*, [15]. In any case, one can only speculate that perhaps ballistic point contacts as 'nanocontacts' might ultimately work, with particular few- \AA -thick semi-conducting nanospacers, and with very clean interfaces.

The suggested experiment concerning the TMR would therefore be analogous to the very recent set-up of Garcia *et al.*, [33], but with a small semi-conducting tip of the above-mentioned kind.

5 Conclusions

We have performed a systematic study of the CPP-GMR and CIP-GMR (i.e. with *Current Perpendicular to the Planes* or *Current in the Planes*, respectively), for systems consisting of two 'ideal leads' attached to two ferromagnetic metallic slabs, which are three monolayers thick, separated by n_s monolayers of non-magnetic (metallic or non-metallic) spacer material. A simple two-band model is used throughout, where in the metallic case one band mimics the s-bands, and the other one the d-bands which are spin-dependent in the ferromagnetic metals, whereas for nonmetallic spacers the two bands describe the valence band and the conduction band, respectively. The s-d-hybridization is taken into account, and is important for our re-

sults. For the metals, and also for the semi-conducting spacer, we use two specific parameter sets, corresponding in the metallic case very roughly to the situation of a Co/Cu/Co-trilayer system with Cu leads, whereas in the non-metallic case the two parameter sets of the spacer distinguish between situations corresponding to an 'indirect' and a 'direct' energy gap, respectively.

The calculations have been performed by very accurate Green's function methods and applied to systems without impurities, with non-magnetic bulk impurities in the spacer, and with magnetic and non-magnetic interface impurities produced by mutual interdiffusion of the atoms near the interface. Within our formalism other situations could also have been treated, e.g. more complicated geometries as (i) the 'constrictions' studied experimentally by Garcia *et al.*, [33], or (ii) quasi-one-dimensional problems, where the potentials are constant within a layer, but random from one layer to the next. The last-mentioned problem has already been extensively studied by J. Mathon, [17], and in two-dimensional systems by one of the present authors, [42]. Also the recent work of Sanvito *et al.* should be mentioned in this broader context.

In all cases the influence of the strength of disorder leads to strong effects, sometimes to an enhanced GMR and sometimes to a reduction. However for different model parameters the outcome can be quite different, which is not astonishing after all, since three conductances are involved in the changes, namely $\Gamma_{\uparrow}^{(++)}$, $\Gamma_{\downarrow}^{(++)}$, and $\Gamma_{\sigma}^{(+-)}$, and the GMR effect is – after all – a difference effect out of these quantities.

So our calculation shows among other results that for the GMR one can hardly avoid extensive calculations for very realistic models of the specific systems considered. Only for the CPP case with impurities in the bulk of a metallic spacer, the GMR seems to be strongly reduced with increasing strength σ_r of the disorder, but only as long as σ_r remains $\lesssim 1$ (Fig. 8 and Fig. 9). In contrast, interface impurities may lead in the same case to a reduction of the GMR for one parameter set (Fig. 10), but to an enhancement for another set (Fig. 11).

One of our main results is perhaps the suggested existence of a drastic *increase* of the GMR with increasing spacer thickness in case of ballistic conductance through a *nonmetallic* spacer, see section 4 above, where we also suggest an experimental realization along the lines of the

recent experiments of Garcia *et al.*, [33].

Acknowledgements

We would like to thank Prof. Dr. P. Bruno, Prof. Dr. P. Weinberger, and Prof. Dr. G. Bayreuther, and the experimentalists around him, for stimulating discussions. S.K. thanks the Humboldt foundation for financial support and the University of Regensburg for its hospitality, and U.K. does the same w.r. to the Polish Academy of Sciences and the Institute of Molecular Physics in Poznań.

References

- [1] M.N. Baibich, J.M. Broto, A. Fert, F. Nguyen Van Dau, F. Petroff, P. Etienne, G. Creuzet, A. Friederich, and J. Chazelas, *Phys. Rev. Lett.* **61**, 2472 (1988).
- [2] G. Binasch, P. Grünberg, F. Saurenbach, and W. Zinn, *Phys. Rev. B* **39**, 4828 (1989).
- [3] S. Toscano, B. Briner, H. Hopster, and M. Landolt, *J. Magn. Magn. Mater.* **114**, L6 (1992).
- [4] B. Briner and M. Landolt, *Z. Phys. B* **97**, 459 (1995).
- [5] D.E. Bürgler, D.M. Schaller, C.M. Schmidt, F. Meisinger, J.M. Kroha, J.M. McCord, A. Hubert, and J.J. Güntherodt, *Phys. Rev. Lett.* **80**, 4983 (1998).
- [6] R. Meservey, P.M. Tedrow, and P. Fulde, *Phys. Rev. Lett.* **25**, 1270 (1970).
- [7] M. Julliere, *Phys. Lett.* **54A**, 225 (1975).
- [8] M.B. Stearns, *J. Magn. Magn. Mater.* **5**, 167 (1977).
- [9] D.J. Monsma, J.C. Lodder, Th.J.A. Popma, and B. Dieny, *Phys. Rev. Lett.* **74**, 5260 (1995).
- [10] S. Datta and B. Das, *Appl. Phys. Lett.* **56**, 665 (1990).

- [11] G.A. Prinz, Physics Today, April issue, p. 58 (1995).
- [12] J.C. Slonczewski, Phys. Rev. B **39**, 6995 (1989).
- [13] J. Mathon, Phys. Rev. B **56**, 11810 (1997).
- [14] W.H. Butler, X.-G. Zhang, and X. Wang, J. Appl. Phys. **81**, 5518 (1997).
- [15] J.M. MacLaren, X.G. Zhang, W.H. Butler, Xindong-Wang, Phys. Rev. B **59**, 5470 (1999).
- [16] E. Yu. Tsybal and D.G. Pettifor, Phys. Rev. B **54**, 15314 (1996).
- [17] J. Mathon, Phys. Rev. B **55**, 960 (1997).
- [18] S. Krompiewski and U. Krey, Europhys. Lett. **44**, 661 (1998)
- [19] Kees M. Schep, Paul J. Kelly, Gerrit E.W. Bauer, Phys. Rev. Lett. **74**, 586 (1995).
- [20] Y. Asano, A. Oguri, J. Inoue, and S. Maekawa, J. Magn. Magn. Mat. **136** L18 (1994); Phys. Rev. B **49**, 12381 (1994)
- [21] I. Mertig, P. Zahn, M. Richter, H. Eschrig, R. Zeller, P.H. Dederichs, J. Magn. Magn. Mater. **151**, 363 (1995).
- [22] The GMR is a *ratio* of at three different conductances, namely Γ_{\uparrow}^{++} , Γ_{\downarrow}^{++} , and Γ_{\uparrow}^{+-} ($= \Gamma_{\downarrow}^{+-}$); so it is on the one hand quite a complex quantity; on the other hand, it is not at all sensitive to changes e.g. of the scattering cross-sections if these leave the *ratio* $(\Gamma_{\uparrow}^{++} + \Gamma_{\downarrow}^{++}) / (2\Gamma_{\uparrow}^{+-})$ invariant. Therefore, changes of the scattering cross-sections may not always lead to changes of the GMR, in particular if the scattering is not explicitly spin-dependent. This can be seen e.g. from the ab-initio calculation of the GMR of small systems by Moser *et al.*, [35], and this has been systematically exploited in the papers of the group of I. Mertig *et al.*, e.g. [21, 23, 24, 25]. In fact, to systematically modify the trends of the GMR, one should try to work with spin-dependent impurities in the nonmagnetic spacer, in which case one may almost *ad libitum* tune the sign of the GMR, see e.g. Fig. 7 in [35].

- [23] P. Zahn, J. Binder, I. Mertig, R. Zeller, P.H. Dederichs, Phys. Rev. Lett. **80** 4309 (1998).
- [24] P. Zahn, I. Mertig, M. Richter, H. Eschrig, Phys. Rev. Lett. **75**, 2996 (1995).
- [25] J. Binder, P. Zahn, I. Mertig, J. Magn. Magn. Mater. **165**, 100 (1997).
- [26] S. Sanvito, C.J. Lambert, J.H. Jefferson, and A.M. Bratkovsky, J. Phys. CM: Condens. Matt. **10**, L691 (1998), and Phys. Rev. B **59**, 11936 (1999).
- [27] P.A. Lee and D.S. Fisher, Phys. Rev. Lett. **47**, 882 (1981).
- [28] Here the following remarks are in order:
a) Calculations have also been performed with 8×8 and 16×16 lattices, but our 10×10 -systems with free boundary conditions in the transverse directions, and ideal leads – i.e. infinite extension in the longitudinal direction – turned out to be the optimal compromise between excessive computing time and quality of the results.
b) Although we consider only single-site impurity potentials, every scattering wave can propagate in all directions, i.e. no component of \vec{k} is generically conserved in the scattering.
- [29] S.L. Cunningham, Phys. Rev. B **10**, 4988 (1974).
- [30] J. Mathon, Murielle Villeret, A. Umerski, R.B. Muniz, J. d’Albuquerque e Castro, and D.M. Edwards, Phys. Rev. B **56**, 11797 (1997).
- [31] From Fig. 4a and Fig. 4b, respectively, in case of the parameters corresponding to Fig. 4a one would expect mainly *positive* group velocities at the Fermi surface, whereas from Fig. 4b *negative* group velocities should dominate. This may be one of the reasons for the different trends observed below.
- [32] Our formalism would of course also allow variations of the geometry, e.g. *nanoconstrictions* instead of the spacer, see the recent experiments of Garcia *et al.* , [33].

- [33] N. Garcia, M. Muñoz, Y.W. Zhao, Phys. Rev. Lett. **82**, 2923 (1999).
- [34] S. Datta, "Electronic transport in mesoscopic Systems", Cambridge University Press, Cambridge (1995).
- [35] A. Moser, U. Krey, A. Paintner, B. Zeller, J. Magn. Magn. Mater. **183**, 272 (1998).
- [36] P. Bruno, H. Itoh, J. Inoue, S. Nonoyama, J. Magn. Magn. Mater. **198-199**, 46 (1999).
- [37] The typical experimental results for the CIP-GMR are in fact significantly smaller than the CPP-GMR, see e.g. the review of Gijs and Bauer, [38], but not as small as in most theoretical calculations, including the present one. However with *magnetic* impurities one should get higher values of the CIP-GMR, see e.g. the already cited paper of Moser *et al.*, [35]. One should also consider at this place the fact that the CIP-GMR is usually measured in the presence of magnetic domains near the interface. There is, however, a recent preprint, [39], where the usual average over many domains is avoided by measuring the CIP-GMR with two ultra-small point contacts. Here one observes in fact experimentally the same small values of the CIP-GMR as calculated theoretically.
- [38] Martin A.M. Gijs, Gerrit E.W. Bauer, Advances in Physics **46**, 285 (1997).
- [39] S.J.C.H. Theeuwen, J. Caro, K.P. Wellock, S. Radelaer, C.H. Marrows, J.B. Hickey, V.I. Kozub, DIMES-preprint cond-mat/9911133
- [40] O. Gebele, Diploma Thesis, University of Regensburg 1998, unpublished.
- [41] J. Mathon, private communication.
- [42] M. Böhm, work in progress.

Tables

Model parameters (i), from overall band-structure				
	Co		Cu	
	E(s)	E(d, σ)	E(s)	E(d)
\uparrow	0.0	-2.6	0.0	-2.6
\downarrow	0.0	-2.1	0.0	-2.6
Fermi energy: $E_F = 3D - 2.8$				
Hopping integrals: $t_s = 3D - 1, t_d = 3D - 0.2, t_{sd} = 3D0.3$				

Table 1: Model parameters (i); metallic spacer

Model parameters (ii), from overall behaviour of the DOS				
	Co		Cu	
	E(s)	E(d, σ)	E(s)	E(d)
\uparrow	0.0	-1.0	0.0	-1.0
\downarrow	0.0	-0.2	0.0	-1.0
Fermi energy: $E_F = 3D0.0$				
Hopping integrals: $t_s = 3D - 1, t_d = 3D - 0.2, t_{sd} = 3D1.0$				

Table 2: Model parameters (ii); metallic spacer

		'Isolator 1'	
		$t_s \equiv -1.0, t_d \equiv -0.2, t_{sd} \equiv 0.3$	
small gap :	$0.025eV$	$E_s = -8.77$	$E_d = -1.60$
intermediate gap :	$0.17eV$	$E_s = -8.85$	$E_d = -1.55$
large gap :	$3.4eV$	$E_s = -9.77$	$E_d = -0.60$

Table 3: Parameter set (iii): Non-metallic spacer; 'indirect energy gap'; $E_F = -2.8$; the set of the first line was always used in the paper, with $t_s \equiv -1, t_d \equiv -0.2, t_{sd} \equiv 0.3$ throughout.

	'Isolator 2'	
	$t_s \equiv -1, t_d = 0^*), t_{sd} \equiv 0.3$	
energy gap at $k_{[111]} = 0.814$: $1.0eV$	$E_s = 2.50$	$E_d = -2.85$
energy gap at $k_{[111]} = 1.888$: $1.0eV$	$E_s = 0.00$	$E_d = -2.80$
energy gap at $k_{[111]} = 3.066$: $1.0eV$	$E_s = -4.0$	$E_d = -2.80$

Table 4: Parameter set (iv): non-metallic spacer; 'direct energy gap'; $E_F = -2.8$; the arrow in Fig. 5 denotes the position of the minimal energy difference $E_c(\vec{k}) - E_v(\vec{k})$; the set of the first line was always used in the paper; $t_s \equiv -1$ and $t_{sd} \equiv 0.3$ throughout, as before,^{*)} and $t_d = -0.2$ for the hopping between two neighbouring metal atoms; whereas, if at least one of the two atoms were nonmetallic, this time $t_d = 0$ was assumed, so that the dispersion of the valence band in the r.h.s. of Figure 5 is solely caused by $t_s \equiv -1$ and the on-site s-d-hybridization $t_{sd} \equiv 0.3$.

Figures

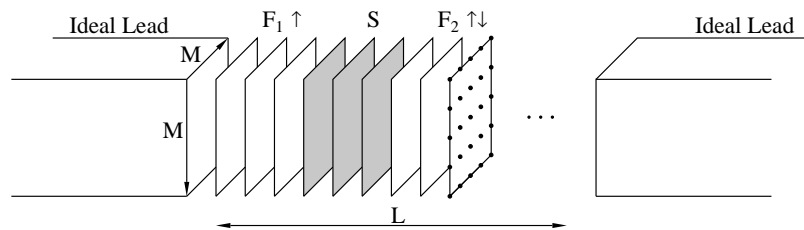


Figure 1: Schematic plot of our systems for the CPP-geometry

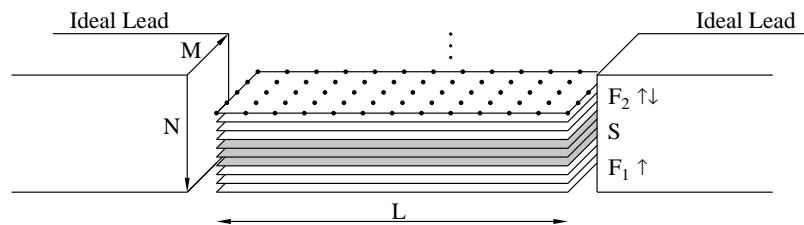


Figure 2: Schematic plot of our systems for the CIP-geometry

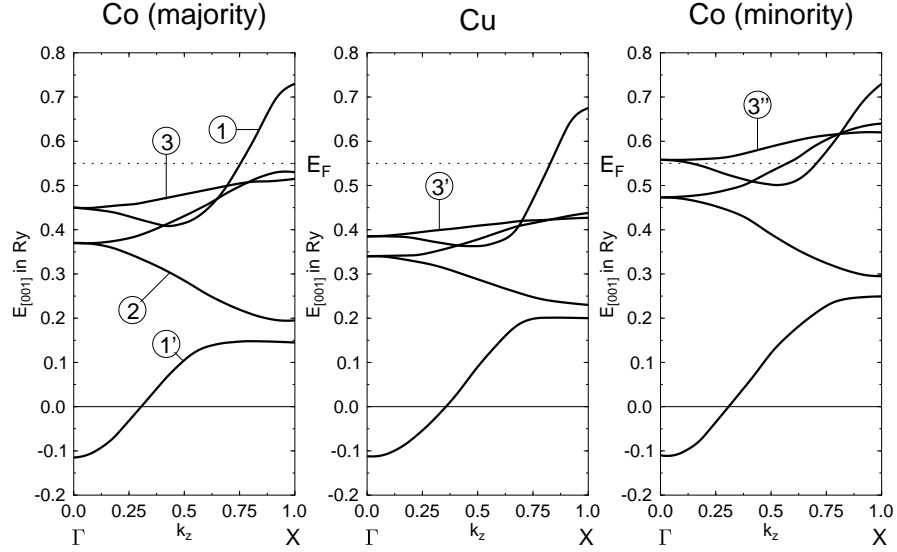


Figure 3: Realistic band-structure of Co and Cu according to [30]. Note the similarity of Cu and Co_\uparrow bands

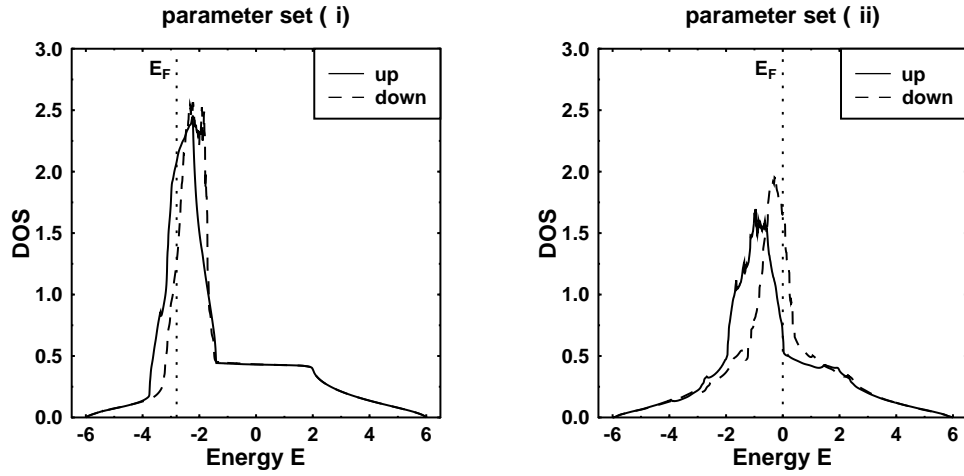


Figure 4: Densities of states for the magnetic metals, for models (i) and (ii)

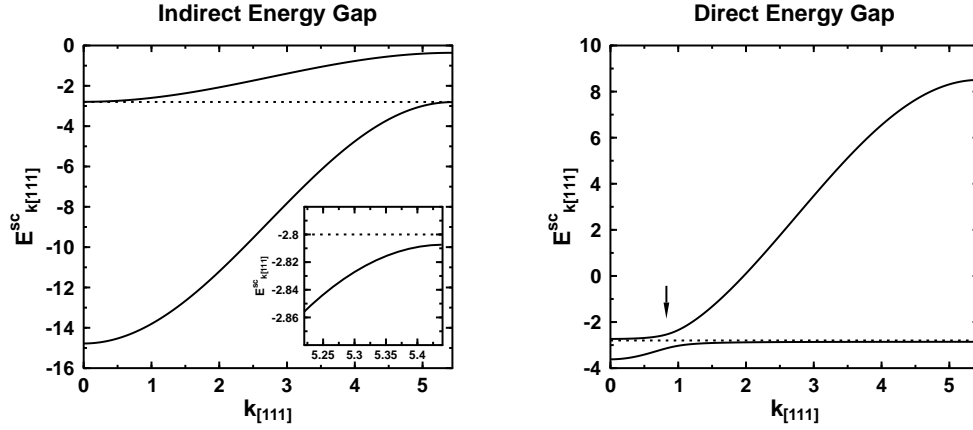


Figure 5: Band-structure of the non-metallic spacers (iii) and (iv); $E_F = -2.8$; on the left h.s. the band structure of model (iii) is shown, with an 'indirect energy gap' from the upper edge of the valence band at $k_{111} = \sqrt{3}\pi$ to the lower edge of the conduction band at $\vec{k} = 0$, which is two times the energy distance to E_F (see the inset); the r.h.s. is for model (iv) with a 'direct gap' represented by the arrow.

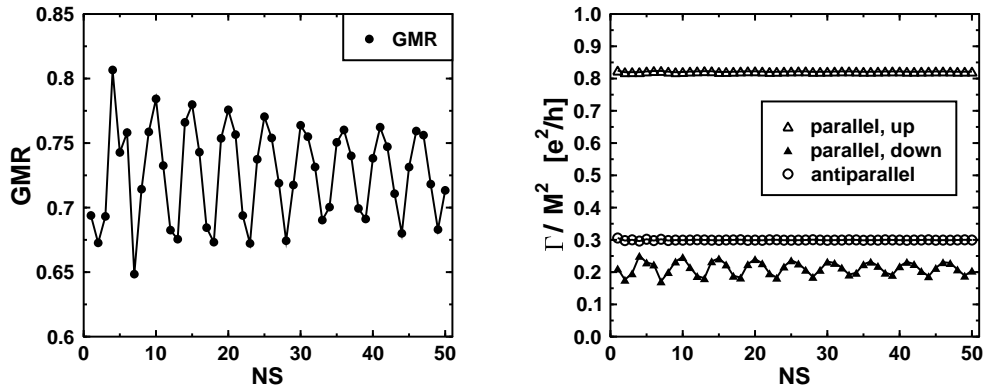


Figure 6: k-space calculation, CPP, system (i)

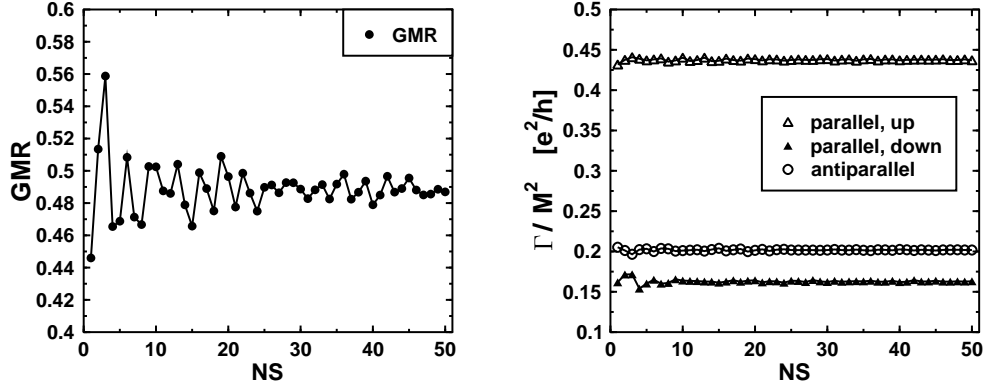


Figure 7: k-space calculation, CPP, system (ii)

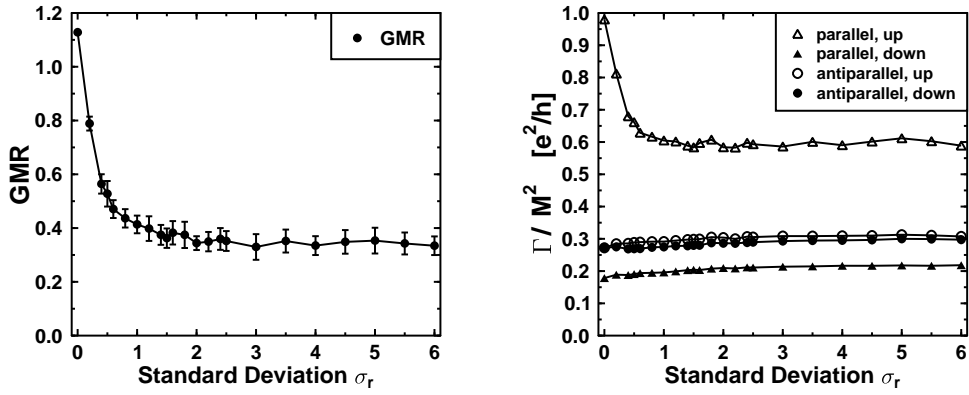


Figure 8: x-space calculation, CPP, system (i), bulk impurities; the standard-deviation σ_r of Eq. (9) characterizes the 'strength of disorder'; 20 samples per point

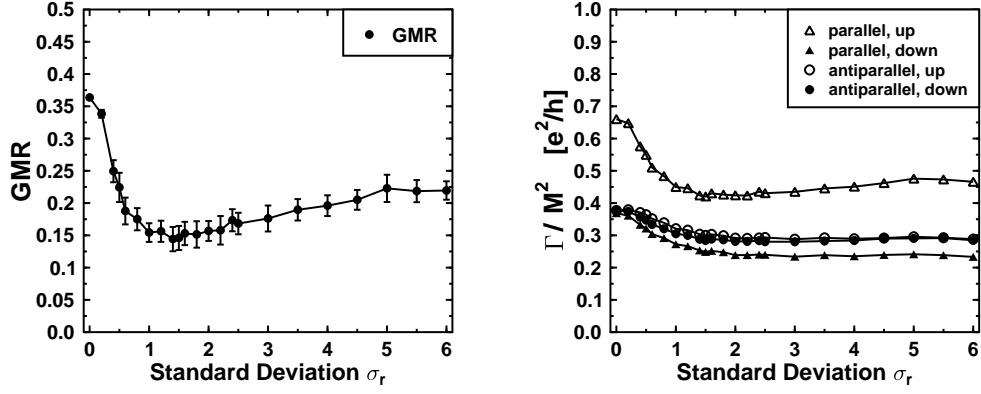


Figure 9: x-space calculation, CPP, system (ii), bulk impurities; the standard deviation σ_r of Eq. (9) characterizes the 'strength of disorder'; 20 samples per point

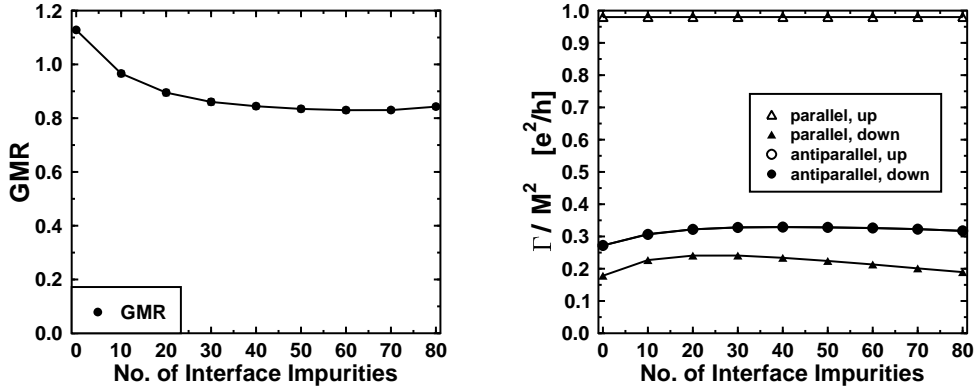


Figure 10: x-space calculation, CPP; system (i); interface impurities; 100 samples per point

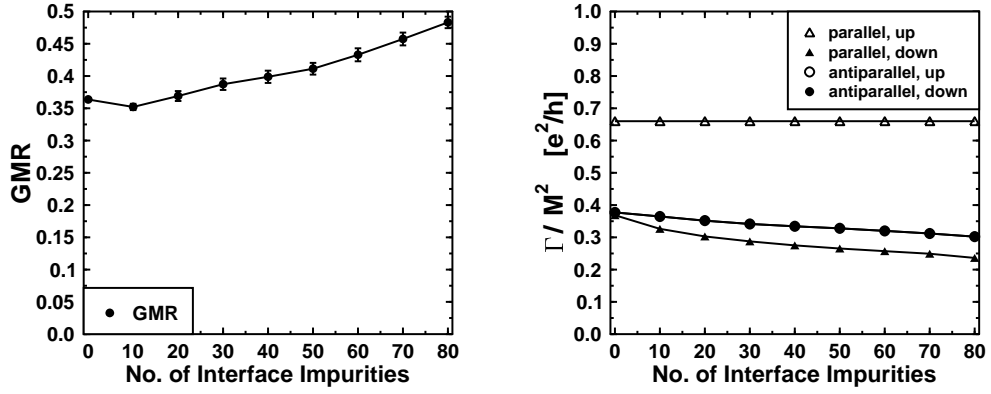


Figure 11: x-space calculation; CPP; system (ii); interface impurities; 100 samples per point

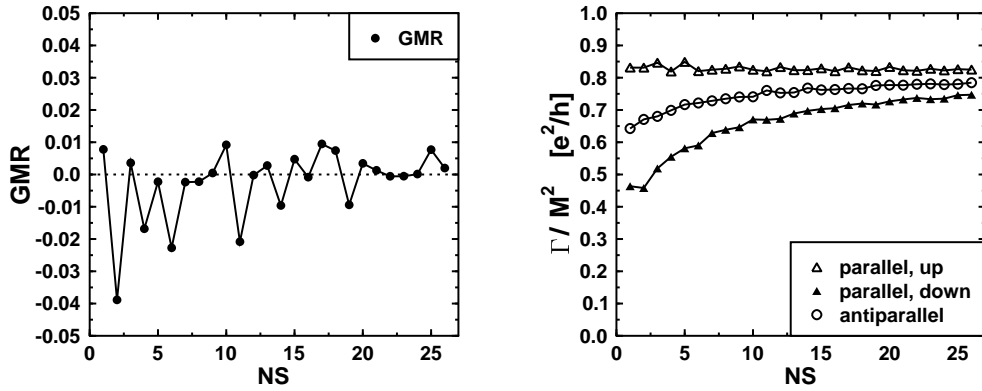
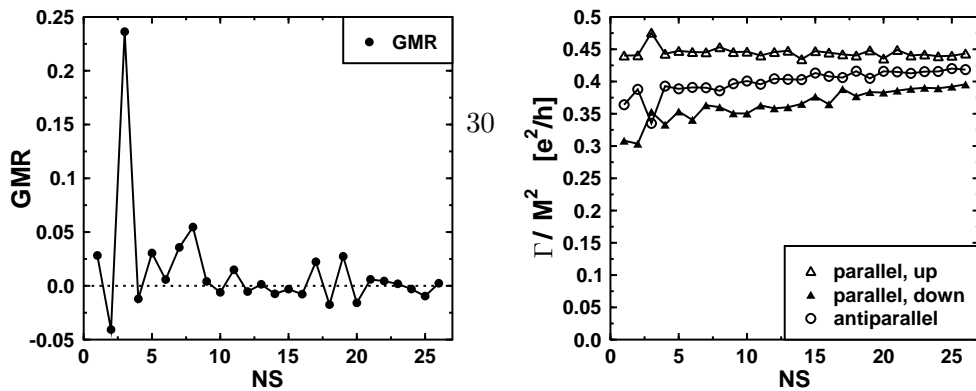


Figure 12: x-space calculation, CIP, system (i); no impurities



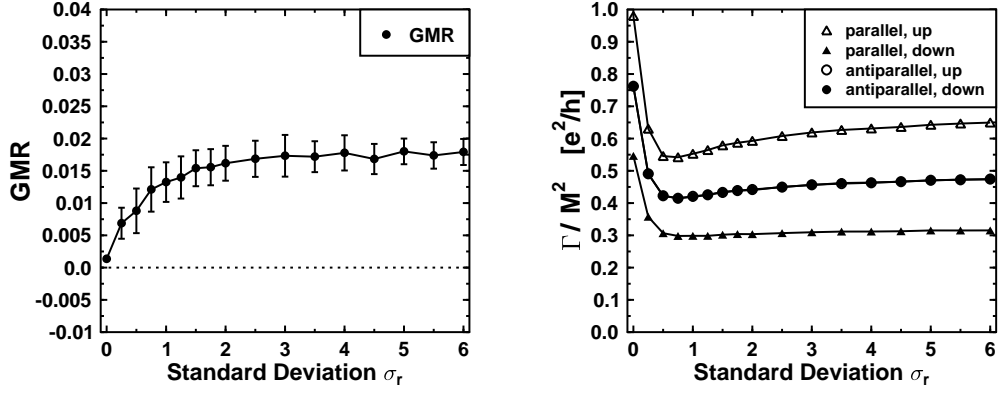


Figure 14: x-space calculation; CIP; system (i); bulk impurities; the 'standard deviation' σ_r of Eq. (9) characterizes the 'strength of disorder'; 100 samples per point

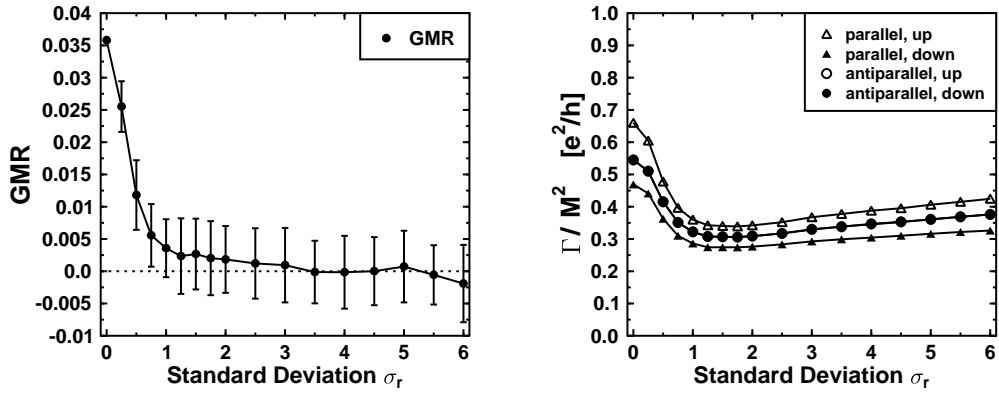


Figure 15: x-space calculation; CIP; system (ii); bulk impurities; the 'standard deviation' σ_r of Eq. (9) characterizes the 'strength of disorder'; 100 samples per point

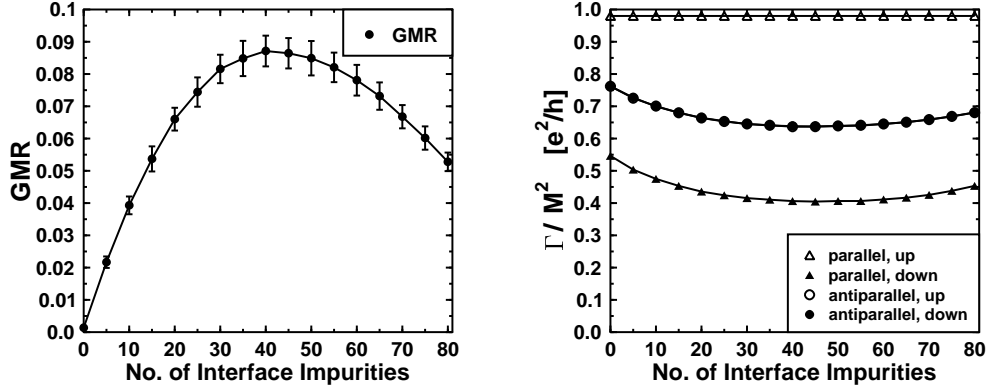


Figure 16: x-space calculation; CIP; system (i); interface impurities; 100 samples per point

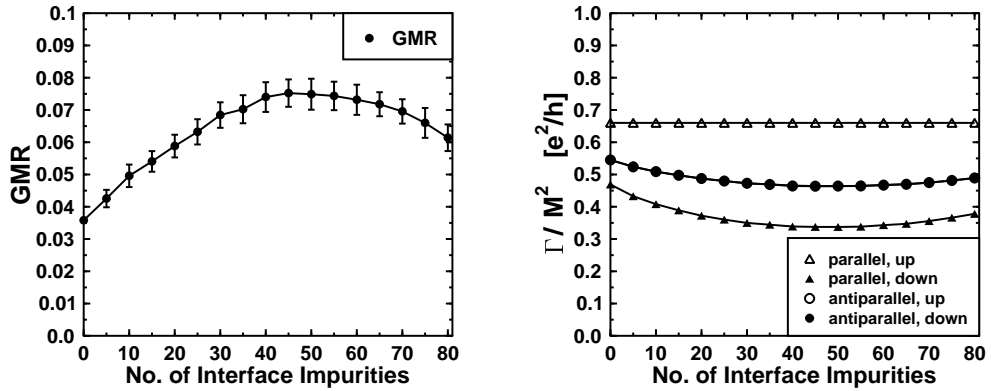


Figure 17: x-space calculation; CIP; system (ii); interface impurities; 100 samples per point

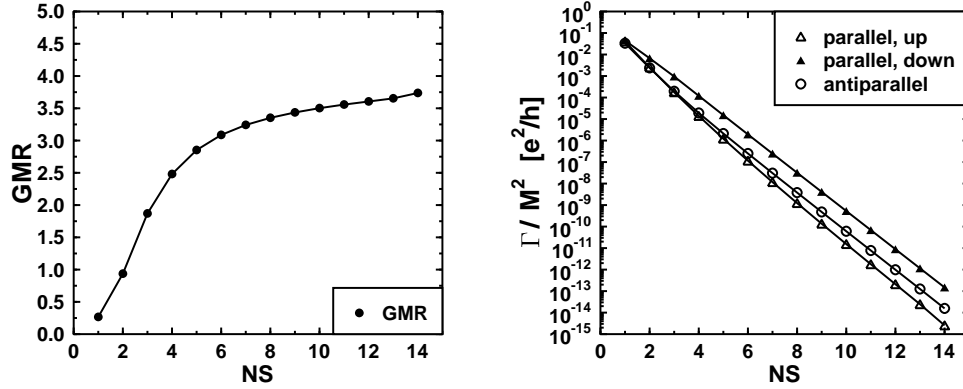


Figure 18: CPP-GMR for non-metallic spacer (iv), i.e. with *direct* gap; $NF_1 = NF_2 = 3$; parameters corresponding to line 1 in Table 4; no impurities

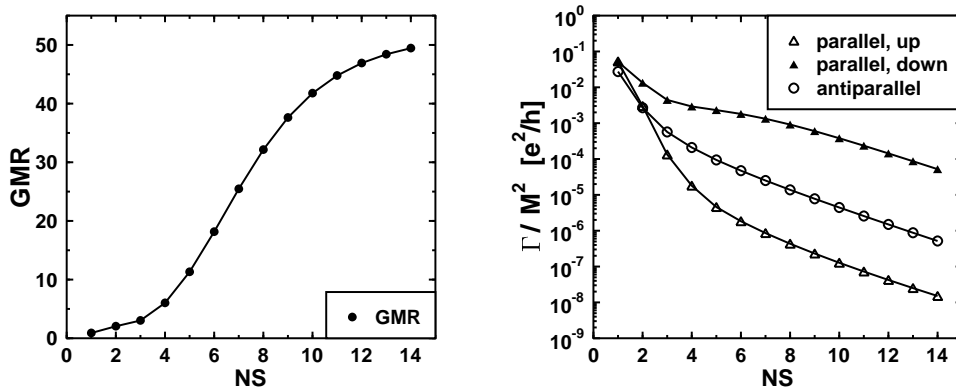


Figure 19: CPP-GMR for non-metallic spacer (iii), i.e. with *indirect* gap; $NF_1 = NF_2 = 3$; parameters corresponding to line 1 in Table 3; no impurities